

GluN2A-Selective NMDA Receptor Antagonists: Mimicking the U-Shaped Bioactive Conformation of TCN-201 by a [2.2]Paracyclophane System

Ruben Steigerwald,^[a, b] Tsung-Han Chou,^[c] Hiro Furukawa,^[c] and Bernhard Wünsch^{*[a, b]}

Under physiological conditions, *N*-Methyl-*D*-Aspartate (NMDA) receptors play a crucial role for synaptic plasticity, long-term potentiation and long-term depression. However, overactivation of NMDA receptors can result in excitotoxicity, which is associated with various neurological and neurodegenerative diseases. The physiological properties of NMDA receptors are strongly dependent on the GluN2 subunit incorporated into the heterotetrameric NMDA receptor. Therefore, subtype selective NMDA receptor modulators are of high interest. Since prototypical GluN2A-NMDA receptor antagonists TCN-201 and its MPX-analogs adopt a U-shaped conformation within the binding pocket, paracyclophanes were designed containing the phenyl rings in an already parallel orientation. Docking studies

of the designed paracyclophanes show a similar binding pose as TCN-201. [2.2]Paracyclophanes with a benzoate or benzamide side chain were prepared in four-step synthesis, respectively, starting with a radical bromination in benzylic 1-position of [2.2]paracyclophane. In two-electrode voltage clamp experiments using *Xenopus laevis* oocytes transfected with cRNAs for the GluN1-4a and GluN2A subunits, the esters and amides (conc. 10 μ M) did not show considerable inhibition of ion flux. It can be concluded that the GluN2A-NMDA receptor does not accept ligands with a paracyclophane scaffold functionalized in benzylic 1-position, although docking studies had revealed promising binding poses for benzoic acid esters and benzamides.

Introduction

Glutamate receptors play a vital role in the mammalian central nervous system. They are divided into G-protein coupled metabotropic glutamate receptors (mGluRs) and glutamate-gated ion channels referred to as ionotropic glutamate receptors (iGluRs). *N*-Methyl-*D*-aspartate (NMDA) receptors are iGluRs which play a significant role in development, physiology, and disease.^[1]

The NMDA receptor is a heterotetrameric complex with an alternating subunit arrangement in a 1-2-1-2 fashion.^[2] Each subunit can be divided into four domains. The extracellular amino terminal domain (ATD), the extracellular ligand binding domain (LBD), the transmembrane domain (TMD) and the

intracellular carboxy-terminal domain (CTD). Each domain contributes to the mechanism of action of the NMDA receptor, i.e., the opening and closing of the cation channel.

NMDA receptors show a high diversity due to a large number of subunits that form the functional receptor. Seven subunits termed GluN1, GluN2A–D, and GluN3A–B encoded by seven genes are known.^[3] The structure of the NMDA receptor is further diversified by the existence of eight splice variants of the GluN1 subunit, which result from alternative splicing of Exon5. The GluN1 subunits without the additional 21 amino acids are termed GluN1-1a to 4a and GluN1 subunits with these amino acids are termed GluN1-1b to 4b.^[4] The presence or absence of Exon5 affects functional properties including channel gating kinetics and pH sensitivity.^{[5][6]} In addition to dimeric NMDA receptors, trimeric NMDA receptors with three different subunits were found and analyzed by Cryo-EM.^[7]


NMDA receptors are activated, when two criteria are met simultaneously: concurrent binding of the endogenous ligands glycine and (*S*)-glutamate at their respective binding sites at the LBD and membrane depolarization, which relieves the Mg²⁺ block. Therefore, NMDA receptors are referred to as coincidence detectors.^[8,9] Upon activation and opening of the receptor channel, the cations Na⁺, K⁺ and Ca²⁺ can cross the cell membrane according to their concentration gradients.


Due to the high conductivity of Ca²⁺ ions, the NMDA receptor plays a crucial role in synaptic plasticity and memory. Long-term potentiation (LTP) and long-term depression (LTD) greatly depend on elevated intracellular Ca²⁺ concentration.^[10,11,12] However, an excess of intracellular Ca²⁺ ions caused by overactivation of the NMDA receptor can trigger

[a] R. Steigerwald, Prof. Dr. B. Wünsch
Chemical biology of ion channels (Chembion)
Westfälische Wilhelms-Universität Münster
Corrensstraße 48, 48149 Münster (Germany)
E-mail: wuensch@uni-muenster.de

[b] R. Steigerwald, Prof. Dr. B. Wünsch
Institut für Pharmazeutische und Medizinische Chemie
Westfälische Wilhelms-Universität Münster
Corrensstraße 48, 48149 Münster (Germany)

[c] Dr. T.-H. Chou, Prof. Dr. H. Furukawa
W.M. Keck Structural Biology Laboratory
Cold Spring Harbor Laboratory
New York, NY 11724 (USA)

 Supporting information for this article is available on the WWW under <https://doi.org/10.1002/cmdc.202200484>

 © 2022 The Authors. ChemMedChem published by Wiley-VCH GmbH. This is an open access article under the terms of the Creative Commons Attribution Non-Commercial License, which permits use, distribution and reproduction in any medium, provided the original work is properly cited and is not used for commercial purposes.

apoptosis. This phenomenon is referred to as excitotoxicity and is associated with numerous conditions such as stroke, status epilepticus as well as neurodegenerative diseases including Parkinson's, Alzheimer's, and Huntington's disease.^[13–16] Therefore, the NMDA receptor can be a relevant target for drug intervention against neuro excitotoxicity. To alleviate excitotoxicity, a number of means to inhibit the NMDA receptor channel activities need to be pursued.

NMDA receptor subtypes contribute differently to the progression of various diseases. Therefore, it is of high interest to target NMDA receptor subtypes selectively with the aim to control pathophysiological conditions but maintain physiological processes.

Ligands of the NMDA receptor can be divided into four groups based on their binding sites: ligands of the glycine binding site, ligands of the glutamate binding site, open channel blockers, and allosteric modulators. The first three groups of ligands bind to regions which are well conserved among NMDA receptor subunits making it difficult to achieve subtype selectivity. Consequently, allosteric modulators appear to be the most promising ligands to selectively address specific NMDA receptor subtypes.

Among all GluN2-containing NMDA receptors, GluN2A-NMDA receptors show fast channel opening kinetics with high Ca^{2+} conductivity resulting in the highest ion currents among all GluN2-NMDA receptors.^[17] Furthermore, they exhibit the highest open probability and fastest deactivation kinetics as well as the highest sensitivity towards the voltage-dependent Mg^{2+} block.^[18] GluN2A-NMDA receptors are predominantly found in the CNS and in certain peripheral tissues.^{[19][20]}

In a high-throughput screening, sulfonamide TCN-201 (1, Figure 1) was identified as potent NMDA receptor ligand. Whole-cell patch-clamp electrophysiology showed the selective binding of 1 to GluN2A-NMDA receptors.^[21] At low extracellular glycine concentration, TCN-201 prevents glycine from binding to its binding site on the GluN1-subunit preventing the activation of the NMDA receptor. Therefore, TCN-201 belongs to the group of negative allosteric modulators (NAM). However, the modulatory effect of 1 decreases with increasing extracellular glycine concentration and is completely eliminated at a

concentration of 300 μM glycine.^[22] Due to low solubility of TCN-201, the applicability in biological studies proved to be difficult.

TCN-201 (1) was soaked into the crystallized GluN1/2A LBD heterodimer. The obtained X-ray crystal structure confirmed the previously proposed binding site of TCN-201 at the interface of the GluN1/2A heterodimer.^{[23][24]} (Figure 2a) The top view illustrates, that the binding site is located deep in between the dimer interface. (Figure 2b) 1 exhibits an unusual binding conformation adopting a U-shaped or *hairpin*-like π - π stacking motif of the two benzene rings A and B. (Figure 2c).

Volkman *et al.* structurally modified 1 to improve the solubility and glycine-dependency leading to the ligands MPX-004 (2) and MPX-007 (3). (Figure 1) In 2 and 3, the benzene ring in the middle of TCN-201 is replaced by a pyrazine ring and the terminal benzoylhydrazino moiety by a (2-methylthiazol-5-yl)methylamino moiety. These modifications resulted in reduced glycine dependency, increased solubility, and increased potency of both ligands.^[25]

MPX-004 (2) and MPX-007 (3) were also soaked into the crystallized GluN1/2A LBD heterodimer. Both ligands 2 and 3 adopt the same unusual U-shaped or *hairpin*-like π - π stacking motif of the two aryl rings A and B as TCN-201 (1). (Figure 3a and 3b)

The systematic modification of ring C of TCN-201 was reported in 2018. The activity of the modified compounds was tested in two-electrode voltage clamp (TEVC) experiments with oocytes from *Xenopus laevis*. Replacement of the terminal phenyl moiety of TCN-201 by a thiophen-2-yl (4), indol-2-yl (5) or indol-3-yl moiety increased the potency 2.5-fold in comparison to TCN-201.^[26] (Figure 4) Furthermore, replacement of benzene rings A and B by the conformationally constrained [2.2]paracyclophane system was tolerated by the NMDA receptor. In TEVC experiments, the [2.2]paracyclophane 6 (Figure 4) revealed approximately 36% inhibitory activity of TCN-201 (1) at GluN2A-NMDA receptors.^[27]

In the reported series of ligands, the [2.2]paracyclophane system was functionalized at the aromatic ring, as displayed for benzamide 6. To better mimic the *p*-disubstituted ring B of TCN-201, the ring C imitating substituent should be attached to

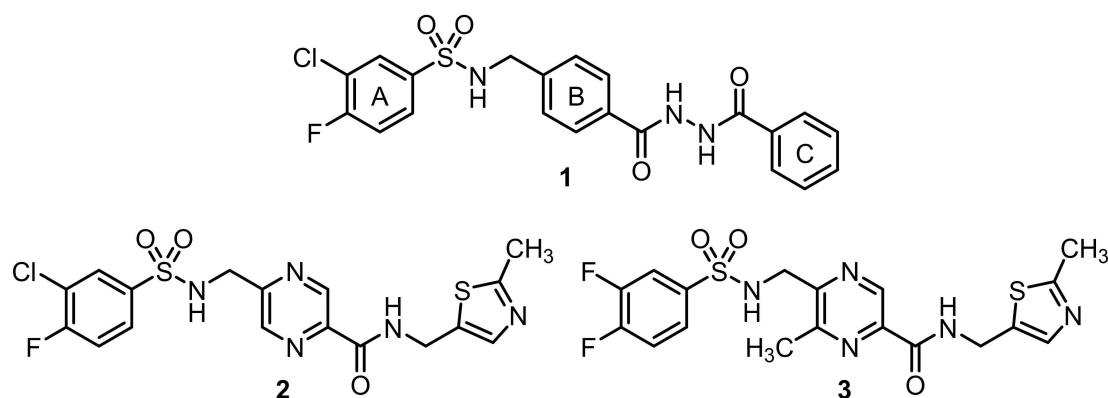


Figure 1. Negative allosteric modulators of the GluN1/2A-NMDA receptor: TCN-201 (1), MPX-004 (2), MPX-007 (3). A, B, and C in the structure of TCN-201 (1) mark the three benzene rings of the molecule.

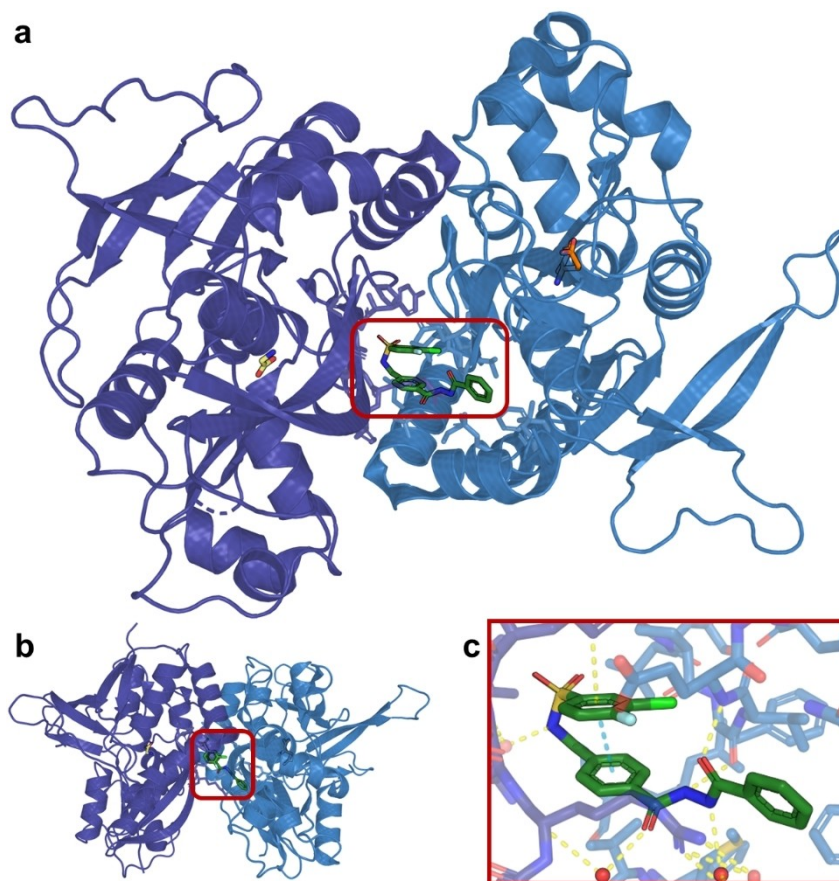


Figure 2. Crystal structure of bound TCN-201 (1, red box) at the GluN1/2A NMDA receptor LBD dimer.^[24] a: side-view of the GluN1/2A-LBD heterodimer, b: top-view of the GluN1/2A-LBD heterodimer, c: magnification of the binding pocket with bound TCN-201 (green). Color code: dark blue: GluN1 subunit; light blue: GluN2A subunit; yellow: glycine; orange: (S)-glutamate. PBD: 5I56; the figures were generated with PyMOL2.

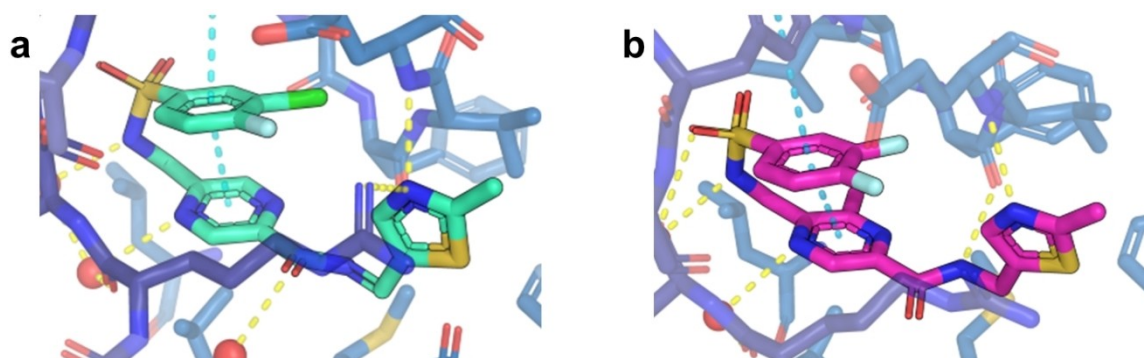


Figure 3. Crystal structure of bound MPX-004 (2) and MPX-007 (3) at the GluN1/2A NMDA receptor LBD dimer.^[24] a: magnification of the binding pocket with bound MPX-004 (cyan), b: magnification of the binding pocket with bound MPX-007 (pink). Color code: dark blue: GluN1 subunit; light blue: GluN2A subunit. PBD: 5I58 (a), 5I59 (b); the figures were generated with PyMOL2.

the aliphatic position of [2.2]paracyclophane. Herein, we wish to report on docking studies, synthesis and biological evaluation of [2.2]paracyclophanes **7** and **8** representing conformational restricted analogs of TCN-201. (Figure 5)

Results and Discussion

Docking studies

Docking studies showed that the conformationally constrained [2.2]paracyclophane system of **7** and **8a** fits well into the binding pocket and is able to mimic the *hairpin*-like conforma-

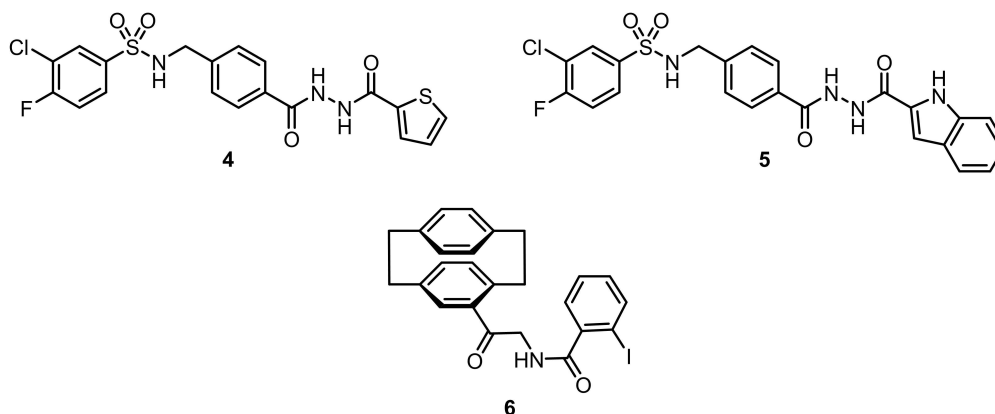


Figure 4. GluN2A-selective NAMs derived from TCN-201.

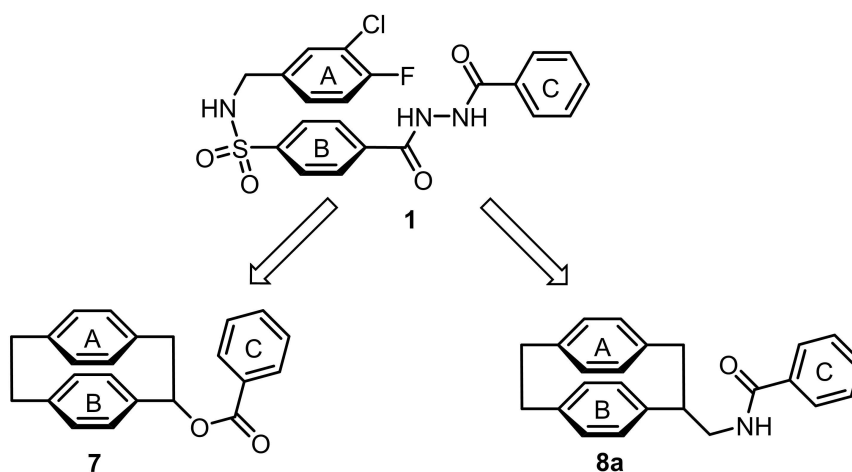


Figure 5. Development of [2,2]paracyclophanes **7** and **8a** as pre-oriented analogs of TCN-201.

tion of TCN-201. (Figure 6) Due to these promising results, the synthesis of [2,2]paracyclophanes of type **7** and **8a** was planned and carried out.

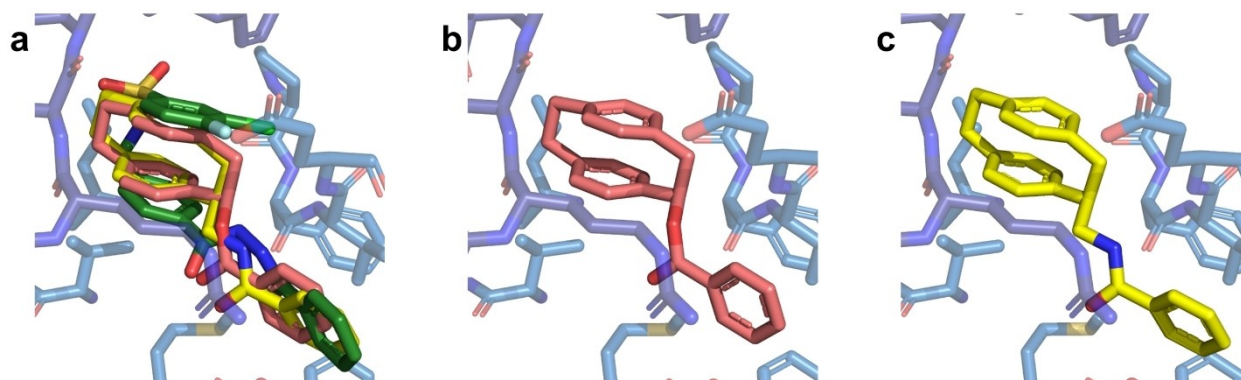


Figure 6. Docking experiments of **7** and **8a** led to a similar binding poses as reported for TCN-201. a: superimposition of docked poses of TCN-201 (**1**, green), **7** (salmon), and **8a** (yellow). b: docking pose of **7** (salmon). c: docking pose of **8a** (yellow). Color code: dark blue: GluN1 subunit, light blue: GluN2A subunit. Docking studies were performed with AutoDock Vina and visualized with PyMOL.^[28,29]

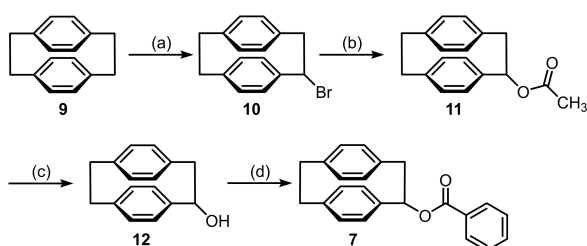
Synthesis of designed [2.2]paracyclophanes

The synthesis of paracyclophane-based TCN-201 analogs **7** and **8** started with [2.2]paracyclophane (**9**). Wohl-Ziegler bromination of **9** with NBS and AIBN in CCl_4 led to the monobrominated paracyclophane **10**. The ester **7** was obtained by conversion of benzyl bromide **10** in a S_N1 -like substitution with AgOAc to yield acetate **11**. Saponification of acetate **11** with LiOH provided the secondary alcohol **12** which was subsequently acylated with benzoyl chloride to obtain ester **7**. (Scheme 1)

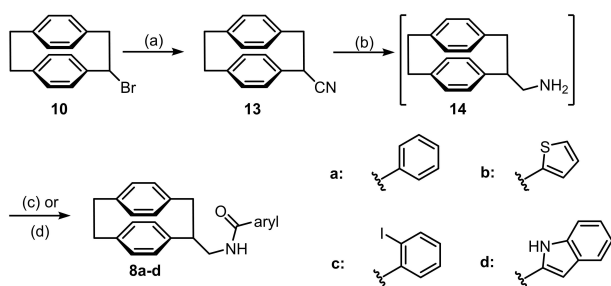
Homologous amides **8** were obtained by reaction of benzyl bromide **10** with CuCN in NMP to obtain nitrile **13**. Pd-catalyzed hydrogenation of nitrile **13** led to the primary amine **14**. Without purification, the primary amine **14** was acylated either with benzoyl chloride in the presence of pyridine or with arenecarboxylic acids in the presence of EDCI/DMAP to obtain arenecarboxamides **8a-d**. (Scheme 2)

Pharmacological evaluation

The GluN2A-NMDA receptor antagonistic activity of the [2.2]paracyclophanes **7**, **11**, and **8a-d** was determined in two-electrode voltage clamp (TEVC) experiments using *Xenopus laevis* oocytes transfected with cRNAs for the GluN1-4a and GluN2A subunits. The ion current was induced by addition of 100 μM glycine and 100 μM (S)-glutamate. Reduction of this ion



Scheme 1. Synthesis of benzoate **7**. Reagents and reaction conditions: (a) NBS, AIBN, CCl_4 , 85 °C, 16 h, 19%. (b) AgOAc, HOAc, 100 °C, 16 h, 36%. (c) LiOH, THF, rt, 82%. (d) benzoyl chloride, CH_2Cl_2 , pyridine, rt, 63%. The substituted [2.2]paracyclophanes represent racemic mixtures.



Scheme 2. Synthesis of arenecarboxamides **8a-d**. Reagents and reaction conditions: (a) CuCN, NMP, 140 °C, 4 h, 25%. (b) H_2 (5 bar), Pd/C, EtOAc, rt, 3 d. (c) benzoyl chloride, CH_2Cl_2 , pyridine, 0 °C, 3 h, 15% (**8a**, two steps). (d) RCO_2H , EDCI, CH_2Cl_2 , DMAP, 0 °C, 2 h, 13% (**8b**), 12% (**8c**), 13% (**8d**), yield over two steps, respectively. The substituted [2.2]paracyclophanes represent racemic mixtures.

current by application of the test compounds was counted as antagonistic activity. The changed membrane currents were normalized to the inhibition of the reference compound TCN-201 (**1**, inhibition = 100%).

At the high concentration of 10 μM , the test compounds **7**, **11**, and **8a-d** exhibited only 3% of inhibitory activity of TCN-201. (Figure 7). Therefore, it can be concluded that none of the tested compounds are viable ligands at the GluN2A-NMDA receptor.

Conclusion

GluN2A-NMDA receptor ligands **7**, **11** and **8a-d** containing a [2.2]paracyclophane moiety were designed to mimic the *hair-pin*-like structure of bound TCN-201 (**1**). For this purpose, the third phenyl ring C was attached to the aliphatic position to mimic the 1,4-disubstituted benzene ring B of TCN-201.

Although docking studies showed promising binding poses for **7** and **8a**, neither the [2.2]paracyclophane based esters **7** and **11** nor the amides **8** showed considerable inhibitory activity at GluN2A-NMDA receptors. We speculate that TCN-201 (**1**), MPX-004 (**2**), and MPX-007 (**3**) can easily reach the binding pocket due to the flexible connections of their aryl moieties. In contrast, in **7**, **8**, and **11** the aryl rings A and B are tightly connected in the [2.2]paracyclophane system and these [2.2]paracyclophanes are no longer able to penetrate into the protein and reach their target binding site.

Experimental Section

Chemistry, general methods

Oxygen and moisture sensitive reactions were carried out under nitrogen, dried with silica gel with moisture indicator (orange gel, VWR, Darmstadt, Germany) and in dry glassware (Schlenk flask or Schlenk tube). Temperature was controlled with dry ice/acetone (−78 °C), ice/water (0 °C), Cryostat (Julabo TC100E-F, Seelbach, Germany), magnetic stirrer MR 3001 K (Heidolph, Schwalbach, Germany) or RCT CL (IKA, Staufen, Germany), together with temperature controller EKT HeiCon (Heidolph) or VT-5 (VWR) and PEG or silicone bath. All solvents were of analytical or technical grade quality. Demineralized water was used. CH_2Cl_2 was distilled from CaH_2 ; THF was distilled from sodium/benzophenone; MeOH was distilled from magnesium methanolate. Thin layer chromatography (tlc): tlc silica gel 60 F_{254} on aluminum sheets (VWR). Flash chromatography (fc): Silica gel 60, 40–63 μm (VWR); parentheses include: fraction size (v) and eluent. Automated flash chromatography: Isolera™ Spektra One (Biotage™); parentheses include: eluent, fractions size was always 20 mL. Melting point: Melting point system MP50 (Mettler Toledo, Gießen, Germany), open capillary, uncorrected. MS: MicroTOFQII mass spectrometer (Bruker Daltonics, Bremen, Germany); deviations of the found exact masses from the calculated exact masses were 5 mDa or less; the data were analyzed with DataAnalysis™ (Bruker Daltonics). NMR: NMR spectra were recorded in deuterated solvents on Agilent DD2 400 MHz and 600 MHz spectrometers (Agilent, Santa Clara CA, USA); chemical shifts (δ) are reported in parts per million (ppm) against the reference substance tetramethylsilane and calculated using the solvent residual peak of the non-deuterated solvent; coupling

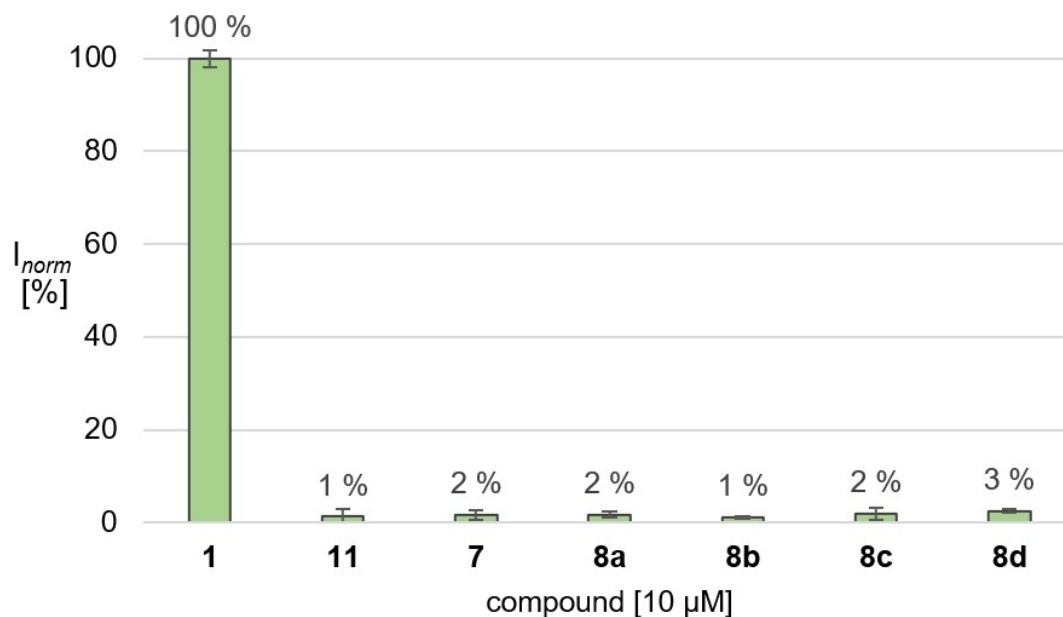


Figure 7. Normalized GluN2A-NMDA receptor inhibition (I_{norm}) of [2.2]paracyclophanes **7**, **8a-d** and **11**. The activity of each compound was measured with three independent oocytes ($n = 3$).

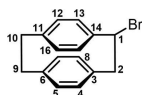
constants are given with 0.5 Hz resolution; assignment of ^1H and ^{13}C NMR signals was supported by 2-D NMR techniques where necessary. IR: FT/IR Affinity⁻¹ spectrometer (Shimadzu, Düsseldorf, Germany) using ATR technique.

HPLC method for the determination of the purity

Equipment 1: Pump: L-7100, degasser: L-7614, autosampler: L-7200, UV detector: L-7400, interface: D-7000, data transfer: D-line, data acquisition: HSM-Software (all from Merck Hitachi, Darmstadt, Germany); Equipment 2: Pump: LPG-3400SD, degasser: DG-1210, autosampler: ACC-3000T, UV-detector: VWD-3400RS, interface: DIO-NEX UltiMate 3000, data acquisition: Chromeleon 7 (equipment and software from Thermo Fisher Scientific, Lauenstadt, Germany); column: LiChrospher[®] 60 RP-select B (5 μm), LiChroCART[®] 250–4 mm cartridge; flow rate: 1.0 mL/min; injection volume: 5.0 μL ; detection at $\lambda = 210$ nm; solvents: A: demineralized water with 0.05% (V/V) trifluoroacetic acid, B: CH_3CN with 0.05% (V/V) trifluoroacetic acid; gradient elution (% A): 0–4 min: 90%; 4–29 min: gradient from 90% to 0%; 29–31 min: 0%; 31–31.5 min: gradient from 0% to 90%; 31.5–40 min: 90%. Unless otherwise mentioned, the purity of all test compounds is greater than 95%.

Synthetic procedures

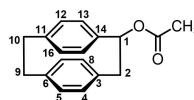
rac-1-Bromo[2.2]paracyclophane (**10**)^[30]



[2.2]Paracyclophane (3.00 g, 14.4 mmol), *N*-bromosuccinimide (3.37 g, 18.9 mmol) and azobisisobutyronitrile (118 mg, 0.7 mmol) were added into a Schlenk tube and dissolved in CCl_4 (50 mL). The reaction mixture was stirred overnight at 85 °C. After cooling to rt, the reaction mixture was filtered, and the solvent was evaporated

in vacuo. The residue was purified by flash chromatography (2 x cyclohexane : ethyl acetate = 100:0 → 95:5; 2x *n*-hexane : cyclohexane = 100:0 → 60:40). Colorless solid, mp 119 °C, yield 770 mg (19%). $\text{C}_{16}\text{H}_{15}\text{Br}$ (287.2 g/mol). TLC: $R_f = 0.29$ (cyclohexane/ethyl acetate 95:5, detection: 254 nm). ^1H NMR (600 MHz, CDCl_3): δ [ppm] = 2.93–3.04 (m, 2H, 9-H, 10-H), 3.16–3.23 (m, 2H, 9-H, 10-H), 3.32 (dd, $J = 14.2/7.2$ Hz, 1H, 2-H), 4.03 (dd, $J = 14.2/9.0$ Hz, 1H, 2-H), 5.19 (dd, $J = 9.0/7.2$ Hz, 1H, 1-H), 6.39 (dd, $J = 7.9/1.8$ Hz, 1H, 8-H), 6.41 (dd, $J = 7.9/1.8$ Hz, 1H, 7-H), 6.50–6.56 (m, 3H, 12-H, 13-H, 16-H), 6.59 (dd, $J = 7.8/1.8$ Hz, 1H, 5-H), 6.64 (dd, $J = 7.8/1.9$ Hz, 1H, 4-H), 6.94–6.98 (m, 1H, 15-H). ^{13}C NMR (151 MHz, CDCl_3): δ [ppm] = 35.6 (1 C, C-9), 35.9 (1 C, C-10), 50.1 (1 C, C-2), 51.9 (1 C, C-1), 130.8 (1 C, C-13), 131.3 (1 C, C-16), 131.9 (1 C, C-15), 132.0 (1 C, C-8), 132.6 (1 C, C-5), 134.1 (1 C, C-7), 134.4 (1 C, C-4), 134.9 (1 C, C-12), 137.8 (1 C, C-14), 139.2 (1 C, C-3), 140.5 (1 C, C-6), 142.4 (1 C, C-11). FT-IR: $\tilde{\nu}$ [cm^{-1}] = 2924 (C–H, aliph.), 1589 (C=C, arom.), 1497 (C=C, arom.), 1412 (C=C, arom.). HRMS (APCI): $m/z = 287.0429$ (calcd. 287.0430 for $\text{C}_{16}\text{H}_{15}^{79}\text{Br}$ [$\text{M} + \text{H}$]⁺), $m/z = 289.0413$ (calcd. 289.0409 for $\text{C}_{16}\text{H}_{15}^{81}\text{Br}$ [$\text{M} + \text{H}$]⁺). Purity (HPLC): $t_R = 23.4$ min, purity 81.2%.

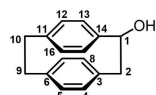
rac-[2.2]Paracyclophan-1-yl acetate (**11**)^[30]



1-Bromo[2.2]paracyclophane (**10**, 502 mg, 1.75 mmol) and AgOAc (319 mg, 1.92 mmol) were dissolved in HOAc (10 mL) under N_2 atmosphere in a Schlenk tube. The resulting mixture was stirred at 100 °C overnight. After cooling to room temperature, the mixture was filtered and washed with H_2O (2 x 10 mL). The pH value of the aqueous phase was adjusted to 6 using NaHCO_3 and the solution was extracted with CH_2Cl_2 (3 x 10 mL). The combined organic layers were dried (Na_2SO_4) and the solvent was evaporated *in vacuo*. The residue was purified by flash chromatography (cyclohexane : ethyl acetate = 100:0 → 80:20). Colorless solid, mp 107 °C, yield 167 mg (36%). $\text{C}_{18}\text{H}_{18}\text{O}_2$ (266.3 g/mol). TLC: $R_f = 0.63$ (cyclohexane : ethyl

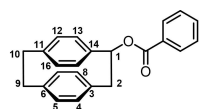
acetate 3:1, detection: 254 nm). ^1H NMR (400 MHz, CDCl_3): δ [ppm]=2.22 (s, 3H, CH_3), 2.89 (ddd, $J=14.1/3.9/0.6$ Hz, 1H, 2-H), 2.99–3.19 (m, 4H, 9-H, 10-H), 3.72 (dd, $J=14.1/9.1$ Hz, 1H, 2-H), 6.14 (dd, $J=9.1/3.9$ Hz, 1H, 1-H), 6.43–6.49 (m, 2H, 4-H, 8-H), 6.50–6.53 (m, 3H, 5-H, 7-H, 13-H), 6.56–6.60 (m, 2H, 12-H, 16-H), 6.80 (dt, $J=8.1/1.3$ Hz, 1H, 15-H). ^{13}C NMR (101 MHz, CDCl_3): δ [ppm]=21.5 (1 C CH_3), 35.6 (1 C, C-10), 35.8 (1 C, C-9), 45.2 (1 C, C-2), 77.4 (1 C, C-1), 129.6 (1 C, C-15), 130.2 (1 C, C-13), 132.8 (1 C, C-5), 132.9 (1 C, C-7), 133.2 (1 C, C-4), 133.4 (1 C, C-8), 133.8 (1 C, C-16), 133.9 (1 C, C-12), 137.4 (1 C, C-14), 137.6 (1 C, C-3), 140.4 (1 C, C-6), 141.6 (1 C, C-11), 170.6 (1 C, C=O). FT-IR: $\tilde{\nu}$ [cm^{-1}]=2920 (C–H, aliph.), 1732 (C=O), 1370 (CH_3), 1238 (C–O–C). HRMS (APCI): $m/z=267.1365$ (calcd. 267.1380 for $\text{C}_{18}\text{H}_{19}\text{O}_2$ [$\text{M}+\text{H}$] $^+$). Purity (HPLC): $t_{\text{R}}=21.8$ min, purity 98.4%.

rac-[2.2]Paracyclophan-1-ol (12)^[30]



Ester **11** (42 mg, 0.16 mmol) was dissolved in THF (5 mL) and the solution was stirred at rt. LiOH (16.8 mg, 0.7 mmol) was dissolved in H_2O (3 mL) and added dropwise to the reaction mixture. After complete conversion monitored by TLC, H_2O (20 mL) was added, the aqueous layer was extracted with CH_2Cl_2 (3×15 mL), the combined organic layer was dried (Na_2SO_4) and the solvent was removed *in vacuo*. Colorless solid, mp 229 °C, yield 29.3 mg (82%). $\text{C}_{16}\text{H}_{16}\text{O}$ (224.3 g/mol). TLC: $R_{\text{f}}=0.41$ (cyclohexane : ethyl acetate 3:1, detection: 254 nm). ^1H NMR (600 MHz, CDCl_3): δ [ppm]=2.89 (dd, $J=13.9/3.6$ Hz, 1H, 2-H), 3.02–3.15 (m, 4H, 9-H, 10-H), 3.65 (dd, $J=13.8/8.9$ Hz, 1H, 2-H), 5.32 (dd, $J=8.9/3.6$ Hz, 1H, 1-H), 6.39–6.46 (m, 3H, 7-H, 8-H, 13-H), 6.49 (m, 5-H, 12-H), 6.60 (td, $J=7.8/2.0$ Hz, 2H, 4-H, 16-H), 6.93 (dd, $J=8.0/1.9$ Hz, 1H, 15-H). ^{13}C NMR (151 MHz, CDCl_3): δ [ppm]=35.7 (1 C, C-9), 35.8 (1 C, C-10), 47.8 (1 C, C-2), 76.5 (1 C, C-1), 128.9 (1 C, C-15), 129.8 (1 C, C-13), 132.6 (1 C, C-8), 132.7 (1 C, C-12), 133.2 (2 C, C-5, C-7), 133.5 (1 C, C-4), 133.9 (1 C, C-16), 138.4 (1 C, C-3), 140.1 (1 C, C-14), 141.6 (1 C, C-6), 141.6 (1 C, C-11). FT-IR: $\tilde{\nu}$ [cm^{-1}]=3541 (OH), 2920 (C–H, aliph.), 1416 (C=C, arom.). HRMS (APCI): $m/z=225.1251$ (calcd. 225.1274 for $\text{C}_{16}\text{H}_{17}\text{O}$ [$\text{M}+\text{H}$] $^+$). Purity (HPLC): $t_{\text{R}}=18.4$ min, purity 98.6%.

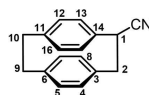
rac-[2.2]Paracyclophan-1-yl benzoate (7)



Alcohol **12** (29.3 mg, 0.13 mmol) was dissolved in a mixture of CH_2Cl_2 and pyridine (5 mL:3 mL) and stirred at rt. Benzoyl chloride (17 μL , 0.15 mmol) was added dropwise to the reaction mixture. After complete conversion monitored by TLC, H_2O (10 mL) and 1 M HCl (10 mL) were added. The aqueous layer was extracted with CH_2Cl_2 (3×10 mL), the combined organic layer was dried (Na_2SO_4) and the solvent was removed *in vacuo*. The residue was purified by preparative TLC (cyclohexane : ethyl acetate = 75:25). Colorless solid, mp 125 °C, yield 26.9 mg (63%). $\text{C}_{23}\text{H}_{20}\text{O}_2$ (328.4 g/mol). TLC: $R_{\text{f}}=0.60$ (cyclohexane : ethyl acetate 3:1, detection: 254 nm). ^1H NMR (600 MHz, CDCl_3): δ [ppm]=3.04–3.18 (m, 5H, 2-H, 9-H, 10-H), 3.83 (dd, $J=14.3/9.1$ Hz, 1H, 2-H), 6.40 (dd, $J=9.1/3.6$ Hz, 1H, 1-H), 6.49–6.53 (m, 2H, 4-H, 5-H), 6.54 (m, 2H, 8-H, 12-H), 6.58 (dd, $J=7.9/1.9$ Hz, 1H, 13-H), 6.61 (dd, $J=8.0/1.9$ Hz, 1H, 16-H), 6.64 (dd, $J=7.9/1.6$ Hz, 1H, 7-H), 6.93 (dd, $J=8.0/1.9$ Hz, 1H, 15-H), 7.51 (m, 2H, 3- H_{phenyl} , 5- H_{phenyl}), 7.59–7.64 (m, 1H, 4- H_{phenyl}), 8.18–8.23 (m, 2H, 2-

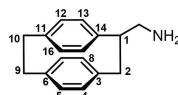
H_{phenyl} , 6- H_{phenyl}). ^{13}C NMR (151 MHz, CDCl_3): δ [ppm]=35.7 (1 C, C-9), 35.8 (1 C, C-10), 45.4 (1 C, C-2), 77.9 (1 C, C-1), 128.6 (2 C, C-3- phenyl , C-5- phenyl), 129.5 (1 C, C-15), 129.9 (2 C, C-2- phenyl , C-6- phenyl), 130.2 (1 C, C-13), 130.6 (1 C, C-1- phenyl), 133.0 (1 C, C-8), 133.1 (1 C, C-12), 133.2 (1 C, C-4- phenyl), 133.3 (1 C, C-4), 133.4 (1 C, C-5), 133.8 (1 C, C-16), 133.9 (1 C, C-7), 137.4 (1 C, C-3), 137.7 (1 C, C-14), 140.4 (1 C, C-6), 141.7 (1 C, C-11), 166.1 (1 C, C=O). FT-IR: $\tilde{\nu}$ [cm^{-1}]=2931 (C–H, aliph.), 1617 (C=O), 1451 (C=C, arom.), 1273 (C–O–C). HRMS (APCI): $m/z=329.1509$ (calcd. 329.1536 for $\text{C}_{23}\text{H}_{21}\text{O}_2$ [$\text{M}+\text{H}$] $^+$). Purity (HPLC): $t_{\text{R}}=24.4$ min, purity 99.6%.

rac-[2.2]Paracyclophan-1-carbonitrile (13)^[31]

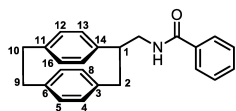


Dry *N*-methylpyrrolidone (NMP, 6 mL) was transferred into a Schlenk flask under nitrogen atmosphere. NMP was heated to 140 °C, before CuCN (707 mg, 7.89 mmol) was added. After 5 minutes, paracyclophan **9** (453 mg, 1.58 mmol) was added, and the resulting mixture was stirred for 4 h at 140 °C. After cooling to room temperature, an ice-cold solution of NaCN (4% wt in H_2O , 50 mL) was added. The formed precipitate was filtered off, dissolved in CHCl_3 (50 mL), the solution was dried (Na_2SO_4) and the solvent was removed *in vacuo*. The crude product was purified by flash chromatography (n-hexane : ethyl acetate = 100:0 \rightarrow 0:50). Remark: Working under dry conditions is crucial. In the presence of H_2O [2.2]Paracyclophan-1-ol (**12**) is formed almost quantitatively. Colorless solid, mp 137 °C, yield 90.6 mg (25%). $\text{C}_{17}\text{H}_{15}\text{N}$ (233.3 g/mol). TLC: $R_{\text{f}}=0.14$ (cyclohexane : ethyl acetate 95:5, detection: 254 nm). ^1H NMR (600 MHz, CDCl_3): δ [ppm]=3.05–3.21 (m, 4H, 9-H, 10-H), 3.37 (dd, $J=13.8/4.6$ Hz, 1H, 2-H), 3.61 (dd, $J=13.7/10.2$ Hz, 1H, 2-H), 4.21 (dd, $J=10.2/4.6$ Hz, 1H, 1-H), 6.41 (dd, $J=7.9/2.2$ Hz, 1H, 13-H), 6.45 (dd, $J=7.8/2.0$ Hz, 1H, 4-H), 6.50–6.57 (m, 3H, 5-H, 7-H, 12-H), 6.61 (dd, $J=7.9/2.1$ Hz, 1H, 16-H), 6.64 (dd, $J=8.0/1.9$ Hz, 1H, 8-H), 6.90 (dd, $J=8.0/2.1$ Hz, 1H, 15-H). ^{13}C NMR (151 MHz, CDCl_3): δ [ppm]=35.74 (1 C, C-10), 35.75 (1 C, C-9), 36.3 (1 C, C-2), 42.7 (1 C, C-1), 121.8 (1 C, CN), 130.8 (1 C, C-15), 132.4 (1 C, C-13), 132.8 (1 C, C-14), 133.1 (1 C, C-4), 133.5 (1 C, C-5), 133.58 (1 C, C-12), 133.62 (1 C, C-7), 133.8 (1 C, C-8), 134.0 (1 C, C-16), 135.3 (1 C, C-3), 141.4 (1 C, C-6), 142.6 (1 C, C-11). FT-IR: $\tilde{\nu}$ [cm^{-1}]=2924 (C–H, aliph.), 2234 (CN), 1497 (C=C, arom.), 1416 (C=C, arom.). HRMS (APCI): $m/z=234.1254$ (calcd. 234.1277 for $\text{C}_{17}\text{H}_{16}\text{N}$ [$\text{M}+\text{H}$] $^+$). Purity (HPLC): $t_{\text{R}}=20.9$ min, purity 95.9%.

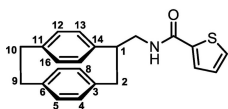
rac-1-(Aminomethyl)[2.2]paracyclophane (14)



Nitrile **14** (94.0 mg, 0.40 mmol) was dissolved in EtOAc (5 mL) and Pd/C 10% (52.5 mg) was added. The reaction mixture was stirred at rt for 3 days under H_2 atmosphere (5 bar) before it was filtered. The solvent was removed under reduced pressure and the crude product was used without further purification. $\text{C}_{17}\text{H}_{19}\text{N}$ (237.4 g/mol).

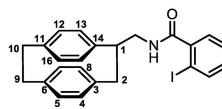
rac-N-[[[2.2]Paracyclophan-1-yl)methyl]benzamide (8a)


Benzoyl chloride (150 μ L, 1.30 mmol) was dissolved in CH_2Cl_2 (2 mL) before pyridine (1 mL) was added under stirring at 0°C . A solution of amine **14** (74 mg) in CH_2Cl_2 (3 mL) was added dropwise. The reaction mixture was stirred at 0°C for 3 h before the ice bath was removed and the solution was allowed to warm up to rt overnight. H_2O (20 mL) was added to obtain a biphasic system. The aqueous layer was separated and extracted with CH_2Cl_2 (3×10 mL), the combined organic layer was dried (Na_2SO_4) and the organic solvent was removed *in vacuo*. The crude product was purified by flash chromatography (cyclohexane:ethyl acetate = 100:0 \rightarrow 75:25) and preparative TLC (cyclohexane : ethyl acetate = 33:67). Colorless solid, mp 175°C , yield over 2 steps 20.6 mg (15%). $\text{C}_{24}\text{H}_{23}\text{NO}$ (341.5 g/mol). TLC: R_f = 0.69 (cyclohexane : ethyl acetate 50:50, detection: 254 nm). ^1H NMR (600 MHz, CDCl_3): δ [ppm] = 2.51 (dd, J = 12.5/6.0 Hz, 1H, 2-H), 2.97–3.07 (m, 2H, 10-H), 3.11–3.21 (m, 2H, 9-H), 3.45–3.56 (m, 2H, 1-H, 2-H), 3.73 (ddd, J = 13.5/10.6/3.8 Hz, 1H, CH_2NH), 4.24 (ddd, J = 13.1/7.5/5.1 Hz, 1H, CH_2NH), 6.27 (s broad, 1H, NH), 6.44 (dd, J = 7.8/1.9 Hz, 1H, 12-H), 6.46–6.59 (m, 6H, 4-H, 5-H, 7-H, 8-H, 13-H, 16-H), 6.63 (dt, J = 8.0/1.2 Hz, 1H, 15-H), 7.36 (dd, J = 8.3/7.1 Hz, 2H, 3- H_{phenyl} , 5- H_{phenyl}), 7.42–7.46 (m, 1H, 4- H_{phenyl}), 7.64–7.69 (m, 2H, 2- H_{phenyl} , 6- H_{phenyl}). ^{13}C NMR (151 MHz, CDCl_3): δ [ppm] = 35.7 (1 C, C-10), 35.7 (1 C, C-9), 41.6 (1 C, C-2), 43.2 (1 C, CH_2NH), 48.5 (1 C, C-1), 127.0 (2 C, C-2 $_{\text{phenyl}}$, C-6 $_{\text{phenyl}}$), 128.7 (2 C, C-3 $_{\text{phenyl}}$, C-5 $_{\text{phenyl}}$), 129.7 (1 C, C-15), 131.5 (1 C, C-4 $_{\text{phenyl}}$), 132.5 (1 C, C-16), 132.6 (1 C, C-13), 132.7 (1 C, C-4), 133.5 (1 C, C-5), 133.9 (1 C, C-12), 134.4 (1 C, C-7), 134.9 (1 C, C-14), 139.1 (1 C, C-3), 139.8 (1 C, C-6), 141.1 (1 C, C-11), 167.7 (1 C, C=O). FT-IR: $\tilde{\nu}$ [cm^{-1}] = 3337 (N–H), 2924 (C–H, aliph.), 1640 (C=O), 1528 (C=C, arom.). HRMS (APCI): m/z = 342.1873 (calcd. 342.1852 for $\text{C}_{24}\text{H}_{24}\text{NO}$ [$\text{M} + \text{H}$] $^+$). Purity (HPLC): t_R = 21.4 min, purity 99.7%.

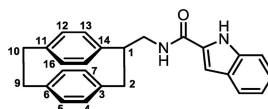
rac-N-[[[2.2]Paracyclophan-1-yl)methyl]-thiophene-2-carboxamide (8b)


Thiophene-2-carboxylic acid (51.9 mg, 0.41 mmol) and amine **14** (68.7 mg) were dissolved in CH_2Cl_2 (5 mL) and the solution was stirred at 0°C . After 5 min, a solution of EDCI (79.9 mg, 0.42 mmol) and DMAP (56.2 mg, 0.46 mmol) in CH_2Cl_2 (5 mL) was added dropwise. The resulting mixture was stirred at 0°C for 2 h before the ice bath was removed and the reaction was allowed to warm up to rt overnight. H_2O (15 mL) was added to obtain a biphasic system. The aqueous layer was separated and extracted with CH_2Cl_2 (3×10 mL). The resulting organic layer was washed with 0.1 M NaOH (3×10 mL), dried (Na_2SO_4) and the organic solvent was removed *in vacuo*. The residue was purified by flash chromatography (cyclohexane : ethyl acetate = 100:0 \rightarrow 70:30). Colorless solid, mp 172°C , yield 13.4 mg (13%). $\text{C}_{22}\text{H}_{21}\text{NOS}$ (347.5 g/mol). TLC: R_f = 0.44 (cyclohexane : ethyl acetate 66:33, detection: 254 nm). ^1H NMR (600 MHz, CDCl_3): δ [ppm] = 2.50 (dd, J = 12.7/6.2 Hz, 1H, 2-H), 2.97–3.06 (m, 2H, 10-H), 3.11–3.21 (m, 2H, 9-H), 3.43–3.55 (m, 2H, 1-H, 2-H), 3.68–3.75 (m, 1H, CH_2NH), 4.19 (ddd, J = 13.2/7.6/5.2 Hz, 1H, CH_2NH), 6.13 (s broad, 1H, CH_2NH), 6.43 (dd, J = 7.8/1.9 Hz, 1H, 12-H), 6.46–6.57 (m, 6H, 4-H, 5-H, 7-H, 8-H, 13-H, 16-H), 6.59–6.64 (m, 1H, 15-H), 6.99 (dd, J = 5.0/3.8 Hz, 1H, 4- $\text{H}_{\text{thiophene}}$), 7.35 (dd, J = 3.8/

1.2 Hz, 1H, 5- $\text{H}_{\text{thiophene}}$), 7.42 (dd, J = 5.0/1.2 Hz, 1H, 3- $\text{H}_{\text{thiophene}}$). ^{13}C NMR (151 MHz, CDCl_3): δ [ppm] = 35.6 (1 C, C-10), 35.7 (1 C, C-9), 41.6 (1 C, C-2), 43.1 (1 C, CH_2NH), 48.5 (1 C, C-1), 127.6 (1 C, C-4 $_{\text{thiophene}}$), 128.0 (1 C, C-5 $_{\text{thiophene}}$), 129.7 (1 C, C-15), 130.0 (1 C, C-3 $_{\text{thiophene}}$), 132.5 (1 C, C-16), 132.6 (1 C, C-13), 132.7 (1 C, C-4), 133.5 (1 C, C-5), 133.9 (1 C, C-12), 134.4 (1 C, C-7), 134.9 (1 C, C-8), 138.86 (1 C, C-14), 138.99 (1 C, C-3), 139.05 (1 C, C-2 $_{\text{thiophene}}$), 139.8 (1 C, C-6), 141.1 (1 C, C-11), 162.1 (1 C, C=O). FT-IR: $\tilde{\nu}$ [cm^{-1}] = 3306 (N–H), 2924 (C–H, aliph.), 1628 (C=O), 1543 (C=C, arom.). HRMS (APCI): m/z = 348.1416 (calcd. 348.1417 for $\text{C}_{22}\text{H}_{22}\text{NOS}$ [$\text{M} + \text{H}$] $^+$). Purity (HPLC): t_R = 21.0 min, purity 99.5%.

rac-2-Iodo-N-[[[2.2]paracyclophan-1-yl)methyl]benzamide (8c)


o-Iodobenzoic acid (111.1 mg, 0.45 mmol) and amine **14** (72.4 mg) were dissolved in CH_2Cl_2 (5 mL) and the solution was stirred at 0°C . After 5 min, a solution of EDCI (83.0 mg, 0.43 mmol) and DMAP (60.2 mg, 0.49 mmol) in CH_2Cl_2 (5 mL) was added dropwise. The resulting mixture was stirred at 0°C for 2 h before the ice bath was removed and the mixture was allowed to warm up to rt overnight. H_2O (15 mL) was added to obtain a biphasic system. The aqueous layer was separated and extracted with CH_2Cl_2 (3×10 mL). The combined organic layer was washed with 0.1 M NaOH (3×10 mL), dried (Na_2SO_4) and the organic solvent was removed *in vacuo*. The residue was purified by flash chromatography (cyclohexane : ethyl acetate = 100:0 \rightarrow 70:30). Colorless solid, mp 148 – 149°C , yield 8.9 mg (12%). $\text{C}_{24}\text{H}_{22}\text{INO}$ (467.4 g/mol). TLC: R_f = 0.42 (cyclohexane : ethyl acetate 66:33, detection: 254 nm). ^1H NMR (600 MHz, CD_3CN): δ [ppm] = 2.53 (dd, J = 12.5/6.2 Hz, 1H, 2-H), 2.96–3.02 (m, 2H, 10-H), 3.08–3.17 (m, 2H, 9-H), 3.45–3.57 (m, 2H, 1-H, 2-H), 3.79–3.91 (m, 2H, CH_2NH), 6.44 (dd, J = 7.8/1.7 Hz, 1H, 12-H), 6.48–6.60 (m, 6H, 4-H, 5-H, 7-H, 8-H, 13-H, 16-H), 6.65 (dd, J = 7.9/1.9 Hz, 1H, 15-H), 6.89 (s broad, 1H, CH_2NH), 7.10 (td, J = 7.7/1.7 Hz, 1H, 4- H_{phenyl}), 7.21 (dd, J = 7.7/1.7 Hz, 1H, 6- H_{phenyl}), 7.36 (td, J = 7.5/1.1 Hz, 1H, 5- H_{phenyl}), 7.85 (dd, J = 7.9/1.1 Hz, 1H, 3- H_{phenyl}). ^{13}C NMR (151 MHz, CD_3CN): δ [ppm] = 35.97 (1 C, C-10), 36.03 (1 C, C-9), 42.1 (1 C, C-2), 43.9 (1 C, CH_2NH), 48.9 (1 C, C-1), 93.1 (1 C, C-2 $_{\text{phenyl}}$), 128.8 (1 C, C-6 $_{\text{phenyl}}$), 129.1 (1 C, C-5 $_{\text{phenyl}}$), 130.9 (1 C, C-15), 131.7 (1 C, C-4 $_{\text{phenyl}}$), 133.2 (1 C, C-16), 133.3 (1 C, C-13), 133.4 (1 C, C-4), 134.3 (1 C, C-5), 134.7 (1 C, C-12), 134.9 (1 C, C-7), 135.5 (1 C, C-8), 140.4 (1 C, C-14), 140.5 (1 C, C-3 $_{\text{phenyl}}$), 140.8 (1 C, C-3), 140.9 (1 C, C-6), 141.3 (1 C, C-11), 144.1 (1 C, C-1 $_{\text{phenyl}}$), 170.3 (1 C, C=O). FT-IR: $\tilde{\nu}$ [cm^{-1}] = 2924 (C–H, aliph.), 1640 (C=O), 1520 (C=C, arom.), 806 (C–I). HRMS (APCI): m/z = 468.0796 (calcd. 468.0819 for $\text{C}_{24}\text{H}_{23}\text{INO}$ [$\text{M} + \text{H}$] $^+$). Purity (HPLC): t_R = 21.9 min, purity 97.4%.

rac-N-(1-Methyl[2.2]paracyclophan)indole-2-carboxamide (8d)


Indole-2-carboxylic acid (89.3 mg, 0.55 mmol) and amine **14** (92.0 mg) were dissolved in CH_2Cl_2 (5 mL) and the mixture was stirred at 0°C . After 5 min, a solution of EDCI (111 mg, 0.58 mmol) and DMAP (61.2 mg, 0.50 mmol) in CH_2Cl_2 (5 mL) was added dropwise. The resulting mixture was stirred at 0°C for 2 h before the ice bath was removed and the mixture was allowed to warm up to rt overnight. H_2O (20 mL) was added to obtain a biphasic system.

The aqueous layer was separated and extracted with CH_2Cl_2 (3 × 10 mL). The combined organic layer was washed with 0.1 M NaOH (3 × 10 mL), dried (Na_2SO_4) and the organic solvent was removed *in vacuo*. The crude product was purified by flash chromatography (cyclohexane:ethyl acetate = 100:0 → 70:30). Colorless solid, mp ~230 °C decomposition, yield 21.0 mg (13%). $\text{C}_{26}\text{H}_{24}\text{N}_2\text{O}$ (380.5 g/mol). TLC: R_f = 0.41 (cyclohexane : ethyl acetate 66:33, detection: 254 nm). ^1H NMR (600 MHz, $\text{DMSO}-d_6$): δ [ppm] = 2.52 (dd, J = 12.8/6.4 Hz, 1H, 2-H), 2.98–3.08 (m, 2H, 10-H), 3.12–3.21 (m, 2H, 9-H), 3.45–3.57 (m, 2H, 1-H, 2-H), 3.77 (ddd, J = 13.7/10.5/3.9 Hz, 1H, CH_2NH), 4.25 (ddd, J = 13.2/7.7/5.3 Hz, 1H, CH_2NH), 6.34 (s broad, 1H, CH_2NH), 6.44 (dd, J = 7.8/1.9 Hz, 1H, 12-H), 6.47–6.58 (m, 6H, 4-H, 5-H, 7-H, 8-H, 13-H, 16-H), 6.63–6.65 (m, 1H, 15-H), 6.67 (dd, J = 2.2/0.9 Hz, 1H, 3- H_{indole}), 7.10 (ddd, J = 8.0/7.0/0.9 Hz, 1H, 6- H_{indole}), 7.24–7.29 (m, 1H, 5- H_{indole}), 7.41–7.45 (m, 1H, 4- H_{indole}), 7.56 (dd, J = 8.1/1.1 Hz, 1H, 7- H_{indole}), 9.24 (s, 1H, $\text{NH}_{\text{indole}}$). ^{13}C NMR (151 MHz, $\text{DMSO}-d_6$): δ [ppm] = 35.65 (1 C, C-10), 35.72 (1 C, C-9), 41.6 (1 C, C-2), 42.8 (1 C, CH_2NH), 48.6 (1 C, C-1), 102.1 (1 C, C-3 $_{\text{indole}}$), 112.0 (1 C, C-4 $_{\text{indole}}$), 120.8 (1 C, C-6 $_{\text{indole}}$), 122.1 (1 C, C-7 $_{\text{indole}}$), 124.7 (1 C, C-5 $_{\text{indole}}$), 127.8 (1 C, C-7a $_{\text{indole}}$), 129.7 (1 C, C-15), 130.7 (1 C, C-2 $_{\text{indole}}$), 132.5 (1 C, C-16), 132.6 (1 C, C-13), 132.7 (1 C, C-4), 133.5 (1 C, C-5), 134.0 (1 C, C-12), 134.5 (1 C, C-7), 134.9 (1 C, C-8), 136.3 (1 C, C-3a $_{\text{indole}}$), 138.8 (1 C, C-14), 138.9 (1 C, C-4), 139.9 (1 C, C-6), 141.2 (1 C, C-11), 161.7 (1 C, C=O). FT-IR: $\tilde{\nu}$ [cm^{-1}] = 3256 (N–H), 2920 (C–H, aliph.), 1636 (C=O), 1547 (C=C, arom.). HRMS (APCI): m/z = 381.1960 (calcd. 381.1961 for $\text{C}_{26}\text{H}_{25}\text{N}_2\text{O}$ [M + H] $^+$). Purity (HPLC): t_R = 21.9 min, purity 95.1%.

Docking studies using AutoDock Vina

AutoDock Vina was used for virtual docking pose screening of compounds **1**, **7** and **8a**. The docking area was assigned visually to cover the binding site of TCN-201 at the GluN1-GluN2A-interface. A grid of 18 × 14 × 20 Å with 0.375 Å spacing was calculated around the docking area for all compounds using AutoGrid. The iterated local search global optimizer algorithm was used to predict the binding free energies for all compounds.

Pharmacological evaluation

The antagonistic activity was tested by two-electrode voltage clamp (TEVC) using *Xenopus laevis* oocytes. cRNAs for the GluN1-4a and GluN2A subunits were injected into defolliculated oocytes. Subsequently, the oocytes were incubated in recovery medium (50% L-15 medium (Hyclone) buffered by 15 mM Na-HEPES at a final pH of 7.4) supplemented with 100 $\mu\text{g mL}^{-1}$ streptomycin, and 100 U mL^{-1} penicillin at 18 °C for 24–48 h. The recording was performed at room temperature in extracellular solution containing 5 mM HEPES, 100 mM NaCl, 0.3 mM BaCl_2 , 10 mM Tricine at final pH 7.4 (adjusted with KOH), and 0.1% DMSO. The agonists solutions were freshly prepared on the day of measurement from 100 mM stock solutions of glycine and glutamate and final concentrations of 100 μM each of the agonists were obtained. The test compound solutions were

prepared from 10 mM DMSO stocks by diluting with agonist solutions and final concentrations of 10 μM for each test compound were obtained. Maximal response current due to NMDA receptor activation was measured with the aid of agarose-tipped micro-electrodes (0.4–0.9 M Ω) at the holding potential of -60 mV. Data were acquired utilizing the program PatchMaster (HEKA) and analyzed by Origin 8 (OriginLab Corp).

After addition of the test compounds, the changed membrane currents were recorded. (Figure 8). The inhibition of test compounds was calculated by the Equation (1).

Equation 1: Calculation of the ion flux inhibition of a test compound.

$$\text{Inhibition} = 1 - \frac{I_c - I_b}{I_a - I_b} \quad (1)$$

Where I_c represents the resting current in presence of the test compound solution, I_b represents the holding current before the agonist addition and I_a represents the current after agonist addition. For comparing the inhibitory activity of the test compounds, the inhibition of each test compound was normalized to the inhibition by the lead compound TCN-201 (1, inhibition = 100%). The normalized inhibition was calculated by the following Equation (2):

Equation 2: Calculation of the normalized inhibition I_{norm} of the test compound related to TCN-201.

$$I_{\text{norm}} (\%) = \frac{\text{Inhibition of compound at } 10 \mu\text{M}}{\text{Inhibition of TCN-201 at } 10 \mu\text{M}} \times 100$$

Abbreviations

AMPA	α -amino-3-hydroxy-5-methyl-4-isoxazolepropionic acid
DMAP	4-Dimethylaminopyridine
EDCI	1-Ethyl-3-(3-dimethylaminopropyl)carbodiimide
iGluR	ionotropic glutamate receptor
LTD	Long term depression
LTP	Long term potentiation
mGluR	metabotropic glutamate receptor
NAM	negative allosteric modulator
NMDA	<i>N</i> -methyl-D-aspartate
NMP	<i>N</i> -methyl-2-pyrrolidone
THF	tetrahydrofuran

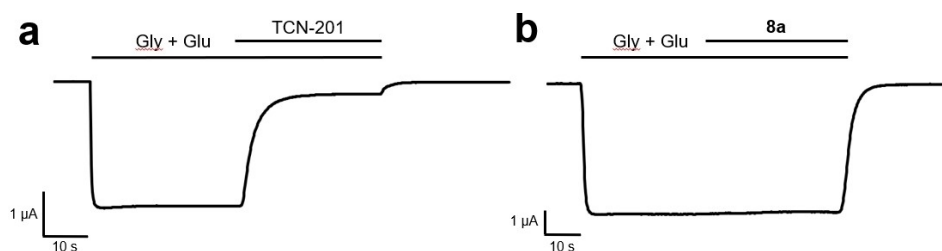


Figure 8. Example traces; a: TCN-201 (**1**), b: *N*-[[2.2]paracyclophan-1-yl)methyl]benzamide (**8a**).

Supporting Information

The Supporting Information contains MS data of all synthesized compounds as well as purity data for all test compounds.

Acknowledgements

This work was supported by the Research Training Group "Chemical biology of ion channels (Chembion)" funded by the Deutsche Forschungsgemeinschaft (DFG), which is gratefully acknowledged. We would like to thank Dr. Max Epstein for helpful discussions regarding the docking studies. HF thanks NIH NS11745, MH085926, Austin's purpose, Robertson funds at Cold Spring Harbor Laboratory, Doug Fox Alzheimer's fund, Heartfelt Wing Alzheimer's fund, and the Gertrude and Louis Feil Family Trust for financial support. Open Access funding enabled and organized by Projekt DEAL.

Conflict of Interest

The authors declare no conflicts of interest.

Data Availability Statement

The data that support the findings of this study are available from the corresponding author upon reasonable request.

Keywords: docking studies · GluN2A · NMDA receptors · [2.2]paracyclophane · TCN-201 · two-electrode voltage clamp

- [1] S. F. Traynelis, L. P. Wollmuth, C. J. McBain, F. S. Menniti, K. M. Vance, K. K. Ogden, K. B. Hansen, H. Yuan, S. J. Myers, R. Dingledine, *Pharmacol. Rev.* **2010**, *62*, 405–496.
- [2] E. Karakas, H. Furukawa, *Science* **2014**, *344*, 992–997.
- [3] H. Chaffey, P. L. Chazot, *Curr. Anaesth. Crit. Care* **2008**, *19*, 183–201.
- [4] H. Li, V. Rajani, L. Han, D. Chung, J. E. Cooke, A. S. Sengar, M. W. Salter, *Proc. Natl. Acad. Sci. USA* **2021**, *118*.

- [5] K. M. Vance, K. B. Hansen, S. F. Traynelis, *J. Physiol.* **2012**, *590*, 3857–3875.
- [6] M. Hollmann, J. Boulter, C. Maron, L. Beasley, J. Sullivan, G. Pecht, S. Heinemann, *Neuron* **1993**, *10*, 943–954.
- [7] S. Bhattacharya, A. Khatri, S. A. Swanger, J. O. DiRaddo, F. Yi, K. B. Hansen, H. Yuan, S. F. Traynelis, *Neuron* **2018**, *99*, 315–328.e5.
- [8] L. Nowak, P. Bregestovski, P. Ascher, A. Herbert, A. Prochiantz, *Nature* **1984**, *307*, 462–465.
- [9] M. L. Mayer, G. L. Westbrook, P. B. Guthrie, *Nature* **1984**, *309*, 261–263.
- [10] R. G. Morris, E. Anderson, G. S. Lynch, M. Baudry, *Nature* **1986**, *319*, 774–776.
- [11] T. V. Bliss, G. L. Collingridge, *Nature* **1993**, *361*, 31–39.
- [12] L. Franchini, N. Carrano, M. Di Luca, F. Gardoni, *Int. J. Mol. Sci.* **2020**, *21*.
- [13] M. Jia, S. A. N. Njapo, V. Rastogi, V. S. Hedna, *CNS Drugs* **2015**, *29*, 153–162.
- [14] S. E. Lakhani, M. Caro, N. Hadzimechalis, *Front. Psychiatry* **2013**, *4*, 52.
- [15] D. R. Zamzow, V. Elias, M. Shumaker, C. Larson, K. R. Magnusson, *J. Neurosci.* **2013**, *33*, 12300–12305.
- [16] S. Davies, D. B. Ramsden, *Mol. Pathol.* **2001**, *54*, 409–413.
- [17] D. J. A. Wyllie, M. R. Livesey, G. E. Hardingham, *Neuropharmacology* **2013**, *74*, 4–17.
- [18] R. J. Clarke, J. W. Johnson, *J. Neurosci.* **2006**, *26*, 5825–5834.
- [19] A. Makhro, Q. Tian, L. Kaestner, D. Kosenkov, G. Faggian, M. Gassmann, C. Schwarzwald, A. Bogdanova, *J. Cardiovasc. Pharmacol.* **2016**, *68*, 356–373.
- [20] B. Merle, C. Itzstein, P. D. Delmas, C. Chenu, *J. Cell. Biochem.* **2003**, *90*, 424–436.
- [21] E. Bettini et al., *J. Pharmacol. Exp. Ther.* **2010**, *335*, 636–644.
- [22] S. Edman, S. McKay, L. J. Macdonald, M. Samadi, M. R. Livesey, G. E. Hardingham, D. J. A. Wyllie, *Neuropharmacology* **2012**, *63*, 441–449.
- [23] K. B. Hansen, K. K. Ogden, S. F. Traynelis, *J. Neurosci.* **2012**, *32*, 6197–6208.
- [24] F. Yi, T.-C. Mou, K. N. Dorsett, R. A. Volkmann, F. S. Menniti, S. R. Sprang, K. B. Hansen, *Neuron* **2016**, *91*, 1316–1329.
- [25] R. A. Volkmann et al., *PLoS One* **2016**, *11*, e0148129.
- [26] J. A. Schreiber, S. L. Müller, S. E. Westphäliger, D. Schepmann, N. Strutz-Seebohm, G. Seebohm, B. Wünsch, *Eur. J. Med. Chem.* **2018**, *158*, 259–269.
- [27] R. Rajan, D. Schepmann, R. Steigerwald, J. A. Schreiber, E. El-Awaad, J. Jose, G. Seebohm, B. Wünsch, *ChemMedChem* **2021**, *16*, 3201–3209.
- [28] O. Trott, A. J. Olson, *J. Comput. Chem.* **2010**, *31*, 455–461.
- [29] J. Eberhardt, D. Santos-Martins, A. F. Tillack, S. Forli, *J. Chem. Inf. Model.* **2021**, *61*, 3891–3898.
- [30] K. C. Dewhirst, D. J. Cram, *J. Am. Chem. Soc.* **1958**, *80*, 3115–3125.
- [31] H. Hopf, M. Psiorz, *Chem. Ber.* **1986**, *119*, 1836–1844.

Manuscript received: September 6, 2022

Revised manuscript received: September 23, 2022

Accepted manuscript online: September 28, 2022

Version of record online: October 13, 2022